Chapter 5

ASTROPHYSICAL APPLICATIONS OF DELBRÜCK SCATTERING: DUST SCATTERED GAMMA RADIATION FROM GRB

5.1. Introduction

There ought to be astrophysical situations where high energy γ-rays interact with an environment containing atomic or molecular dust. For example, a gamma ray burst (*GRB*) is expected to occur in the regions having dense gaseous clouds of their host galaxies [149]. Then, one can talk about the scattering of high energy gamma rays by the atomic nuclei present in the dense cloud. In the present work we restrict ourselves to the elastic scattering only. A photon can be elastically scattered by a nucleus mainly via three different reactions [67]: (i) Delbrück scattering (*DS*), (ii) nuclear Thomson scattering (*NT*) and (iii) nuclear resonance scattering (*NR*). The amplitudes of these reactions depend on scattering angle (θ), atomic number (Z) of the scattering nucleus and the photon-energy (ω). At energies of the order of 0.1 GeV and above, contributions from *NT* and *NR* are negligibly small and therefore the elastic scattering is solely determined by the *DS* amplitudes.

Now, it is a well known fact that there are many evidences in support of the existence of *GRB*s with γ-emissions in the 100 MeV and greater energy range. The *EGRET* (Energetic Gamma Ray Experiment Telescope) onboard *CGRO* (Compton Gamma Ray Observatory) detected five GRBs with emission above100 MeV [150], the *GRID* instrument onboard *AGILE* (an Italian mission) detected few events with energies up to 300 MeV [151], and the Fermi *LAT* (Large Area Telescope) on board *FGST* (Fermi Gamma-ray Space Telescope) has detected 15 *GRB*s with energies greater than100 MeV within18 months of its launch [152].

In the recent past, several attempts have been made to investigate the afterglow emission of *GRB* in different bands like X-ray [153] and optical bands [154] in terms of scattering off the molecular dust. The flux predicted by X-ray models, in which the atomic processes like Rayleigh, Compton and Raman scatterings are considered, resembles most of the observed X-ray afterglows. Such models are thought to be useful for estimating the collimation angle (θ_0) of the *GRB*-jet [153]. The collimation angle θ_0 plays a vital role in global energetics of *GRB* since, for a given burst fluence, the energy release is proportional to $(1-\cos\theta_0)$ and the rate of occurrence of *GRB* varies as θ_0^{-2} [155].

Let us recall that in *DS*, an incident photon is assumed to get converted into a pair of electron and positron in the Coulomb field of the scattering nucleus, and this pair interacts with the nucleus via virtual photons and then recombines to form the final photon having the same energy. The general solution of *DS*, a non-linear quantum eletrodynamic (*QED*) problem, is yet to be established but its solutions valid in some limited regions of photon energies and scattering angles are available [8-10].

In this chapter, the elastic scattering of energetic γ-rays from the dust of a *GRB* is investigated and it has been shown how *DS* plays a vital role in predicting γ-ray flux at the position of the detector immediately after the prompt γ-ray. However, as the Delbrück scattering is highly forward peaked, it acts as an effective scattering mode for an extremely short interval of time just after the burst. It is interesting to note here that most of the issues concerning *GRB* phenomenon have been explained in terms of known processes of atomic physics like bremsstrahlung, Compton scattering, inverse Compton scattering, synchrotron radiation, pair-production, photoelectric-effect, Rayleigh scattering and so on. Probably, the Delbrück scattering is being applied to *GRB* phenomenon for the first time.

5.2. Compton versus Delbrück Scattering at high energy and small angle

At photon-energies ≥100 MeV, Compton scattering (*CS*) off the electrons and *DS* off the nuclei are the major contributor to the scattering process. *DS* is a second order *QED* phenomenon and its cross section goes as $r_o^2(Z\alpha)^4$, α being the fine structure constant and r_o is the classical electron radius. The differential cross section for *DS* at high energy and small angle [35, 36] can be estimated for $m^2/\omega << \Delta << m$ (m is rest mass of an electron, Δ $(=2\omega Sin\theta/2)$ is the momentum transferred to the nucleus) using a simplified relation

$$\frac{d\sigma^D}{d\Omega}=\frac{1}{2}(Z\alpha)^4 r_e^{\,2}\left[a(\omega)+b(\omega)\,\ln(Sin\theta/2)+c(\omega)\{\ln(Sin\theta/2)\}^2\right] \tag{5.1}$$

where,

$$a(\omega)=\left(\frac{\omega}{\pi m}\right)^2\left[0.1187-0.737\,\ln 2\omega+1.21(\ln 2\omega)^2\right], \text{ and}$$

$$b(\omega)=\left(\frac{\omega}{\pi m}\right)^2[\,2.42\ln 2\omega-0.737\,] \text{ and } c(\omega)=1.21\left(\frac{\omega}{\pi m}\right)^2. \tag{5.2}$$

For relatively larger scattering angles satisfying $m << \Delta << \omega$, the asymptotic form of cross section takes the form of Coulomb scattering cross section [9, 42] and can be expressed as

$$\frac{d\sigma^D}{d\Omega} = \frac{1}{4\pi^2}(Z\alpha)^4 r_e^{\,2} \frac{m^2}{\omega^2 Sin^4\theta/2}\left(|g(Z)|^2 + |h(Z)|^2\right) \tag{5.3}$$

where the expressions for $g(Z)$ and $h(Z)$ are given by eqns.(4.6) and (4.7) respectively. Recall that in eqn. (4.7) the function $\psi(x)$ was defined as

$$\psi(x) = d\{\ln\Gamma(x)\}/dx \tag{5.4}$$

The differential cross section for Compton scattering, at small angles such that cosθ ~ 1, can be approximated as

$$\frac{d\sigma^C}{d\Omega} = \frac{1}{2} r_e^{\,2}\left(1 + Cos^2\theta\right) S(\theta, \omega, Z) \tag{5.5}$$

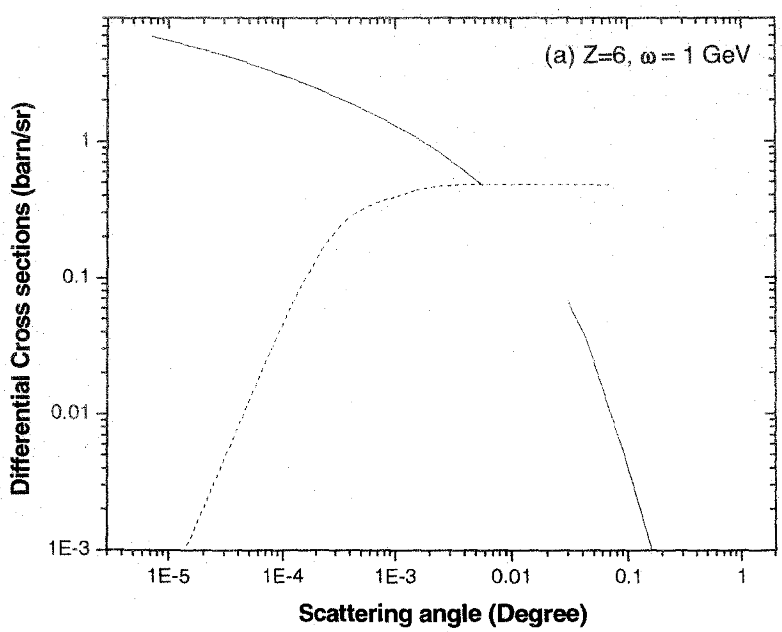

Fig.5.1(a) The dashed and solid curves represent Compton and Delbrück cross section respectively at photon energy of 1 GeV and Z=6. The upper solid curve is for $m^2/\omega \ll \Delta \ll m$ and the lower one for the range of momentum transfer $m \ll \Delta \ll \omega$.

where $S(\theta,\omega,Z)$ is the so called incoherent scattering function (*ISF*). The curves showing the *DS* and *CS* differential cross sections for Z=6 and Z=26 are plotted in Fig. 5.1(a) and 5.1(b) respectively. The values of $S(\theta,\omega,Z)$ are taken from [68].

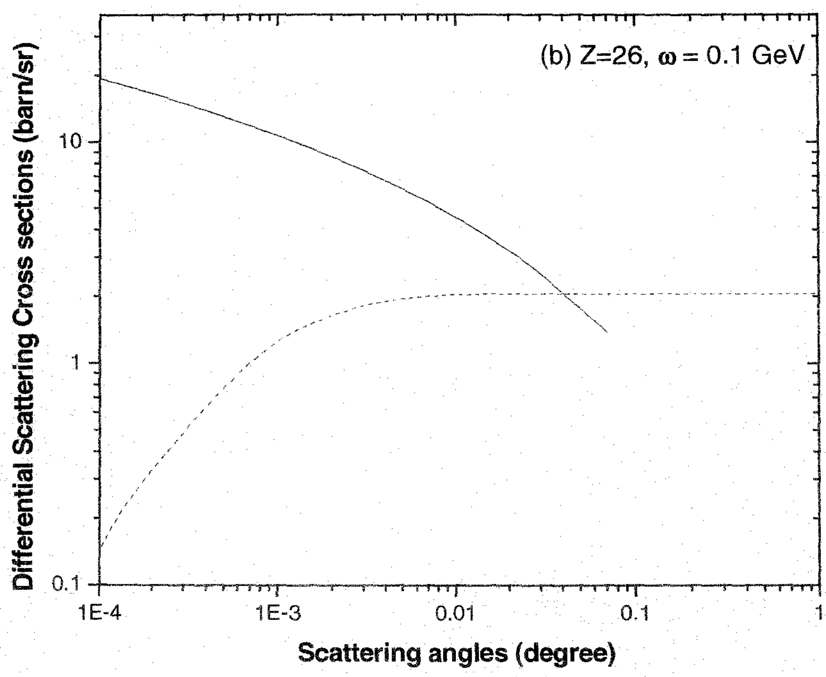

Fig. 5.1(b). Same as Fig. 4.1(a) but for photon energy ω = 0.1 GeV and Z=26. The solid curve has been drawn for the range $m^2/\omega \ll \Delta \ll m$ only.

It is evident from Fig. 5.1(a) that even for a low Z (Z=6) nuclei *DS* cross section at photon energy of 1GeV is substantially more than CS cross section for scattering up to scattering angle of few millidegree and this limit of angle increases to about 0.07 degree for Z=26 and ω=0.1 GeV as shown in Fig. 5.1(b). The break in the solid curve representing *DS* in Fig. 5.1(a) is due to the unavailability of theoretical result corresponding to those momentum transfers.

5.3. Dust scattered gamma emission from *GRB*

In order to illustrate the importance of *DS* phenomenon, particularly in *GRB* and other astrophysical processes in general, a simple model has been assumed in which the *GRB* site is at the center of a spherical dust of uniform density n and radius R. The detector is assumed to be located on the axis of symmetry as shown in the Fig.5.2. The elastically scattered γ-ray at an angle θ will reach the detector D after time $t = t$ whereas the γ-ray without undergoing scattering process will be detected at $t = 0$. The locus of scattering centers making a constant delay will be a paraboloid with its focus at the GRB site. If the host galaxy is at a red shift z then [156]

$$r = \frac{ct}{(1+z)(1-Cos\theta)} \tag{5.6}$$

Let us introduce an angle θ_0 up to which the cross section of *DS* is substantially more than that of *CS* and hence define a corresponding critical time t_1 as

$$t_1 = (R(1+z)(1-Cos\theta_o))/c \tag{5.7}$$

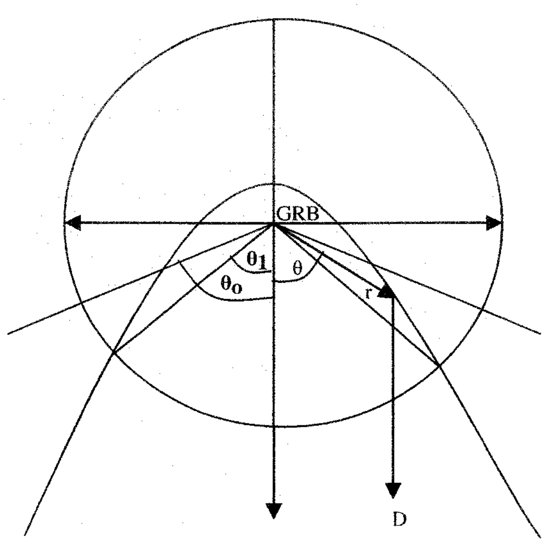

Fig.5.2. Diagram of the model in which GRB is located at the center of a spherical molecular cloud.

The points on the paraboloid, which make the same delay in time t, are constrained within ($r < R$, $\theta < \theta_0$) and the corresponding constraint in terms of scattering angle is $\theta_1 < \theta < \theta_0$, where the critical angle θ_1 is defined as

$$\theta_1 = \cos^{-1}(1 - ct / R(1+z)) \tag{5.8}$$

The scattered and hence delayed γ-ray flux F_γ coming from such a GRB and reaching the detector after time t will, in general, be

$$F_\gamma = S_\gamma n \int_{\theta_1}^{\theta_0} \frac{d\sigma}{d\Omega} \frac{dr}{dt} \, d\Omega \tag{5.9}$$

where S_γ is the γ-ray burst fluence in the energy band [ω_1, ω_2].

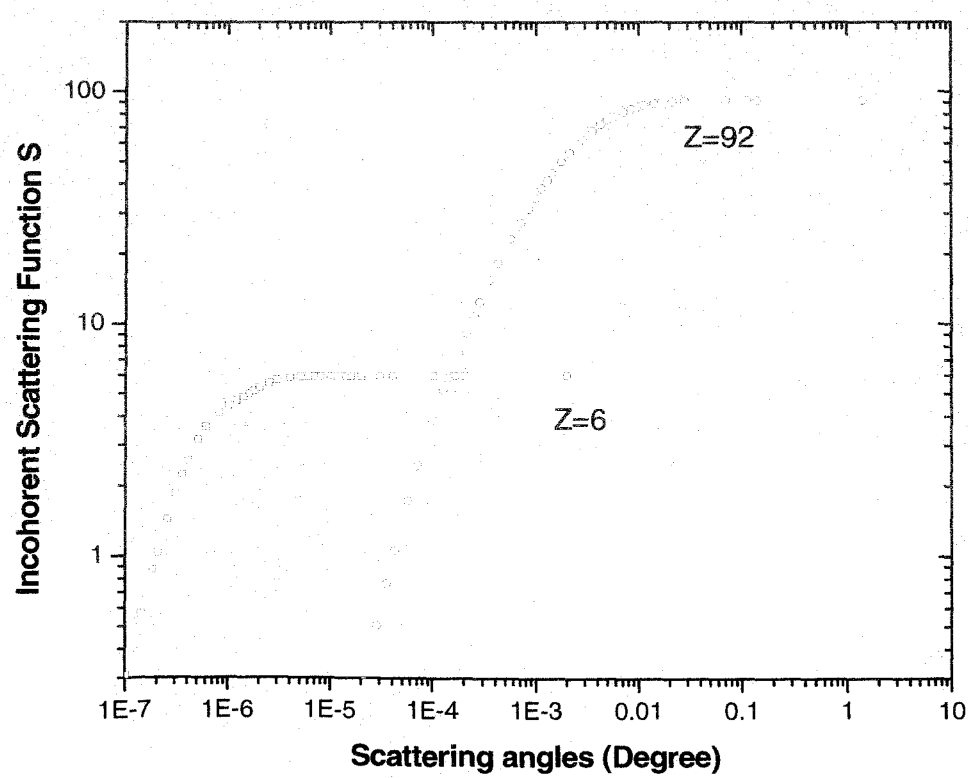

Fig. 5.3.The Incoherent Scattering Function S at different scattering angles for fixed γ-ray energy of 1 GeV. S-values are taken from the tabulation of Hubbell [68].

Assuming the CS to be the only scattering process occurring in the dust of GRB, the γ-ray flux after time t of the burst takes the form

$$F_\gamma^C = S_\gamma n \frac{\pi\, r_o^2}{1+z} c \int_{\theta_1}^{\theta_o} \frac{(1+Cos^2\theta)}{(1-Cos\theta)} S(\theta,\omega,Z)\; Sin\theta\, d\theta \qquad (5.10)$$

The asymptotic value of the ISF $S(\theta,\omega,Z)$ is Z. But, at very small angles $S(\theta,\omega,Z)$ is substantially smaller than Z as seen in Fig.5.3. Substitution of $S(\theta,\omega,Z)=$ Z in eqn. (5.10) will obviously yield larger values of F_γ^C than the actual values at small scattering angles. But, as it is intended to show that the flux corresponding to CS is much less than that of DS at very small angles, taking the higher values of $S(\theta,\omega,Z)$ will not affect the proposition. So, on putting $S(\theta,\omega,Z)=$ Z in eqn.(5.10), one obtains

$$F_\gamma^C = A\,Z\left[\ln\frac{(1-Cos\theta_o)}{(1-Cos\theta_1)} + \frac{1}{2}\left\{(1-Cos\theta_o)^2-(1-Cos\theta_1)^2\right\} - 2\left\{(1-Cos\theta_o)-(1-Cos\theta_1)\right\}\right] \qquad (5.11)$$

where,

$$A = (S_\gamma n\pi\, r_o^2 c)/(1+z)\,. \qquad (5.12)$$

In terms of the critical time t_1 and elapsed time t eqn. (5.11) can be written as

$$F_\gamma^C = A\,Z\left[\,2\ln\frac{t_1}{t} + \left(\frac{(t-t_1)c}{2R(1+z)}\right)\left(4-\frac{(t+t_1)c}{R(1+z)}\right)\right] \qquad (5.13)$$

As stated earlier, for a given γ-ray energy ω and atomic number Z there exists an angle θ_0 beyond which the Delbrück cross section is smaller than Compton cross section. In other words, DS dominates over CS for those scattering angles, i.e., for $\theta < \theta_o$ .For such scattering angles, and also satisfying the condition of momentum transfer for very small scattering angles i.e., $m^2/\omega << \Delta << m$, the Delbrück scattered γ-ray flux F_γ^D is obtained by inserting $d\sigma^D/d\Omega$ from eqn.(5.1) in eqn.(5.9)

$$F_\gamma^D = A\ (\alpha Z)^4 \left[a \ln\frac{(1-Cos\theta_o)}{(1-Cos\theta_1)} + \frac{b}{4}\left(\ln\frac{(1-Cos\theta_o)}{(1-Cos\theta_1)}\right)^2 + \frac{c}{12}\left(\ln\frac{(1-Cos\theta_o)}{(1-Cos\theta_1)}\right)^3 \right]. \quad (5.14)$$

Expressing in terms of elapsed time t the *DS* γ-ray flux F_γ^D will be then

$$F_\gamma^D = A\ (\alpha Z)^4 \left[a \ln\frac{t_1}{t} + \frac{b}{4}\left(\ln\frac{t_1}{t}\right)^2 + \frac{c}{12}\left(\ln\frac{t_1}{t}\right)^3 \right]. \quad (5.15)$$

The *DS* dominated (see Fig. (5.4)) total γ-ray flux F_γ is then given by

$$F_\gamma = F_\gamma^C + F_\gamma^D. \quad (5.16)$$

The components of γ-ray flux, specifically, F_γ^C and F_γ^D have been plotted as a function of time t elapsed after the burst and are depicted in Fig. 5.4.

Taking the value of *GRB* fluence in the energy range 100-600 MeV $S_\gamma \approx 10^{-6}$ erg cm^{-2}, the gas density $n = 10^3$ cm^{-3}, redshift $z = 1$, in eqn.(5.12), one obtains $A \approx 3.7\times10^{-18}$ units. The site of gamma ray burst is considered to be at the center of a spherical cloud of gas having radius $R = 10$ pc and located at redshift $z = 1$. It is assumed that the average atomic number of the molecular cloud is 26. In a real situation it may be less than 26. Although a *GRB* emits electromagnetic radiation in different energy regimes, in the present *GRB* model one focuses on the scattered photons having energies lying within a very small range. In the present illustration the *DS* of photons having average energy ω ≈ 0.1 GeV has been considered. For these choices of parameters the maximum angle θ_0 is found to be about 0.071 degree. It can be seen from Fig.5.4 that, for the present choice of parameters, the *DS* flux is about 1000 times more than the *CS* flux for angles less than

θ_0. Hence, for the first few milliseconds satisfying the condition $\theta < \theta_0$, the *DS* dominated total γ-ray flux F_γ can be approximately written as $F_\gamma \approx F_\gamma^D$.

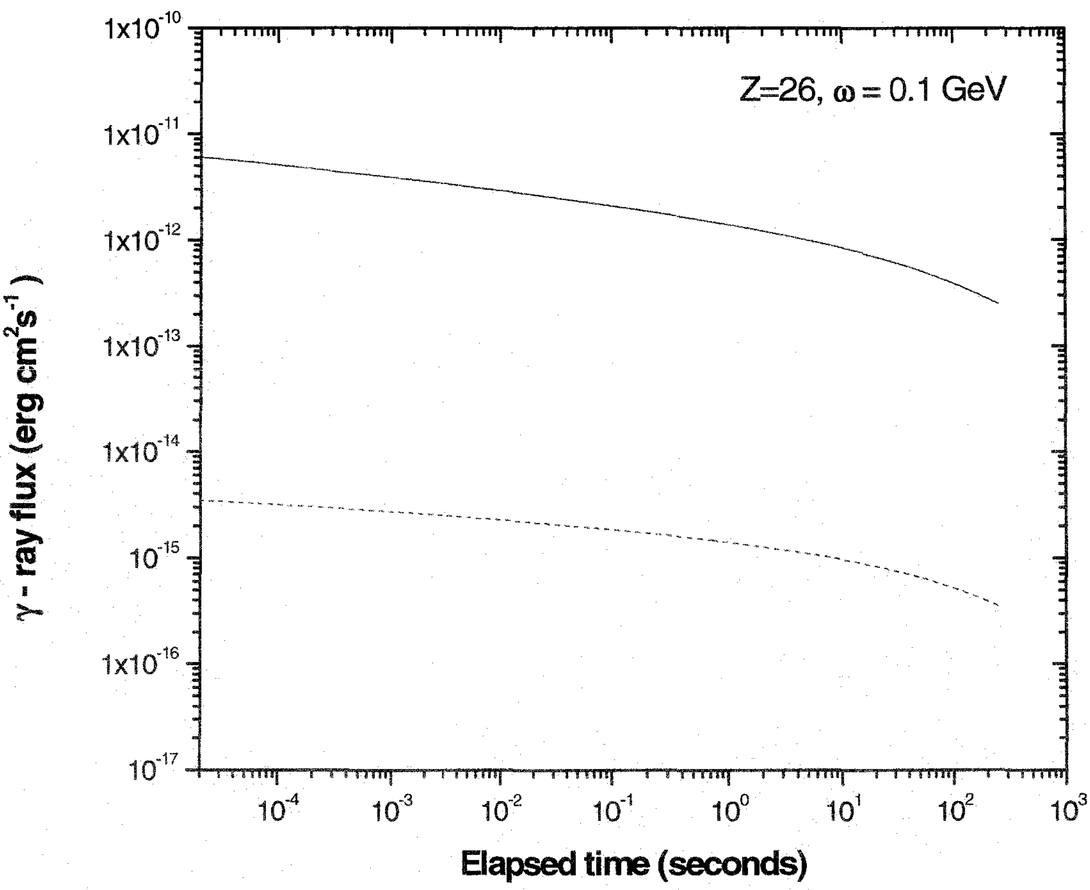

Fig.5.4. The very early flux of a GRB at z =1. Here θ_0=0.071 degree. The solid line and the dashed line correspond to the γ-ray echo of the molecular dust via Delbrück and Compton scatterings respectively. The fluxes are shown up to a time 253 s corresponding up to scattering angle of 0.028 degree. Here R=10 pc, z=1, $S_\gamma = 10^{-6}$ erg cm^{-2}, n = 10^3 cm^{-3}, ω = 0.1 GeV, and Z=26.

When the chosen values of ω and Z are such that the angle θ_0 falls within the range $m << \Delta << \omega$, the Delbrück scattered γ-ray flux for angles $\theta < \theta_0$ is obtained by putting eqn.(5.3) in (5.9). For the sake of clarity θ_1 *and* θ_o will be denoted by θ'_1 *and* θ'_o respectively for the scattering angles falling in the range $m << \Delta << \omega$. The corresponding flux for this case can be expressed as

$$F'^{D}_{\gamma} = A\ (\alpha Z)^4 \frac{m^2}{4\pi^2\omega^2}\left(|g(Z)|^2 + |h(Z)|^2\right)\left[2\left(\frac{1}{(1-Cos\theta'_1)} - \frac{1}{(1-Cos\theta'_0)}\right)\right]. \tag{5.17}$$

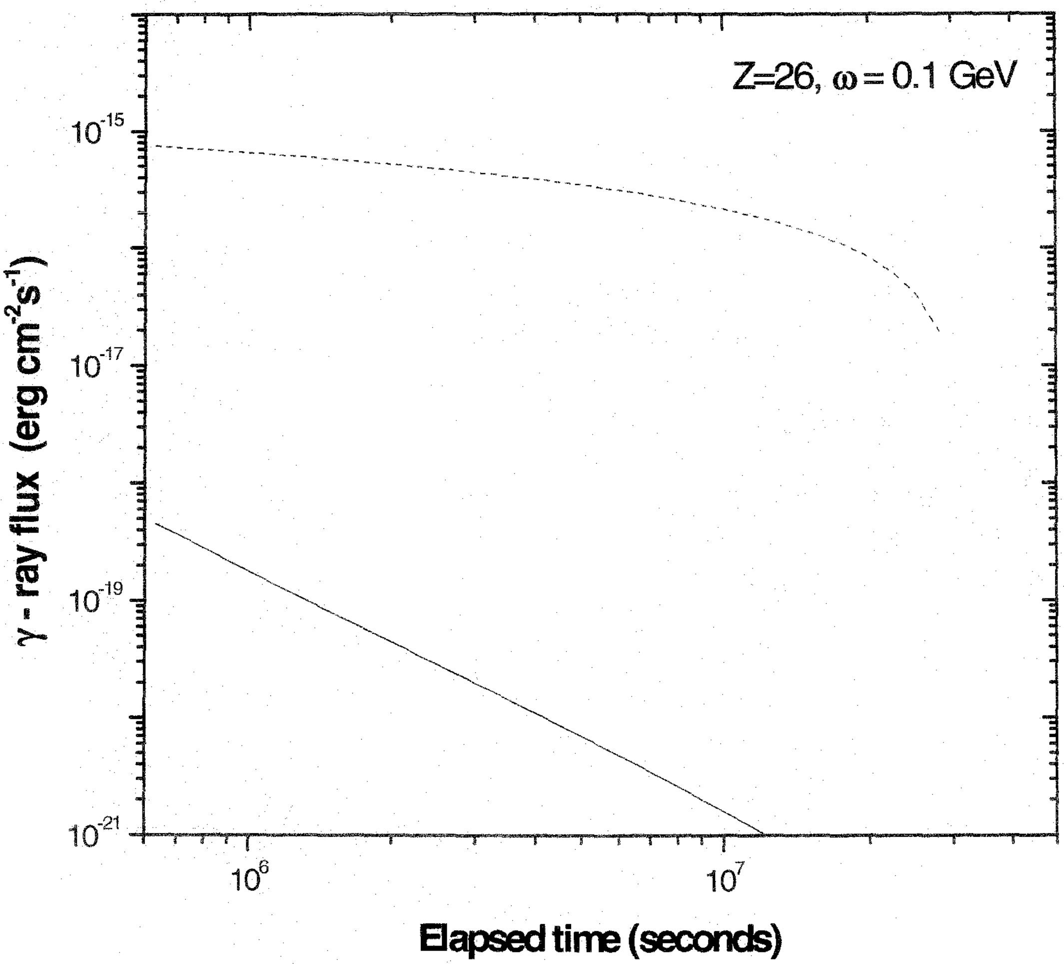

Fig.5.5. The solid line and the dashed line represent the Delbrück scattered and Compton scattered γ-ray flux. Here R=10 pc, z=1, $S_\gamma = 10^{-6}$ erg cm^{-2}, n = 10^3 cm^{-3}, ω = 0.1 GeV, and Z=26.

The eqn. (5.17) can also be expressed in terms of elapsed time. Denoting t and t_1 by t' and t_1' respectively, one can write the flux $F_\gamma'^D$ as

$$F_\gamma'^D = A\ (\alpha Z)^4 \frac{m^2}{4\pi^2\omega^2}\left(|g(Z)|^2 + |h(Z)|^2\right)\left[\frac{2R(1+z)}{c}\left(\frac{1}{(t'} - \frac{1}{t_1'}\right)\right] \tag{5.18}$$

The Compton dominated (see Fig. (5.5)) total γ-ray flux F_γ' is then

$$F_\gamma' = F_\gamma^C + F_\gamma'^D \tag{5.19}$$

The eqn. (5.18) can also be used to calculate the *DS* flux from a *GRB* for any range of scattering angles satisfying the condition $m << \Delta << \omega$. For example, in Fig.5.5, the *DS* flux $F_\gamma'^D$ coming from the same GRB for the angles between $\theta_1' = 1.42^0$ and $\theta_o' = 10^0$ has been plotted. As expected, the *DS* flux is negligible compared to *CS* flux at larger angles. Hence, the total γ-ray flux is mainly dominated by Compton process and hence $F_\gamma' \approx F_\gamma^C$.

If *DS*-dominated total γ-ray flux F_γ, the burst fluence S_γ, the redshift z, and critical time t_1 are measured in an experiment, it will be possible to estimate the molecular gas density n and the critical angle θ_o using eqns. (5.12), (5.13) and (5.15). Similarly, these parameters can be also be estimated from Compton dominated total γ-ray flux F_γ' measured at later times using eqns. (5.12), (5.13) and (5.18).

When the very early scattered γ-ray flux of a GRB is of the type as shown in Fig.5.4, and if energy range and angles satisfy the condition $m^2/\omega << \Delta << m$ then one can estimate the average atomic number Z of the molecular cloud using eqns. (5.12) and (5.15).

5.4. Discussion

The key issue of detectability of Delbrück scattered γ-ray echo from the cloud of a *GRB* will be discussed in this section. Whether such echo is within the capability of the presently operating γ-ray missions *FSGT* and *AGILE* or not depends mainly on the γ-ray burst fluence S_γ of the *GRB*, density n, atomic number Z of the gas and the γ-ray energy ω.

Taking $S_\gamma \approx 10^{-6}$ erg cm^{-2}, n = 10^3 cm^{-3} and z = 1 one gets $A \approx 3.7\times10^{-18}$. This A would make the flux $F_\gamma^D \approx 3.7\times10^{-12}$ erg cm^{-2} s^{-1} at the very beginning of the afterglow. The Fermi *LAT* instrument is expected to detect up to a flux of order 10^{-9} erg cm^{-2} s^{-1}. So, normally, the chances of observing Delbrück scattered γ-ray echo from a *GRB* using Fermi *LAT* is almost nil. However, in the event of a *GRB* with unusually high γ-ray fluence (say 10^{-4} erg cm^{-2}), chances of which are extremely rare, the detection of the Delbrück echo looks possible with the Fermi *LAT*. But, we can be optimistic that the future generation gamma-ray telescopes would be able to see such photons.

Although *DS* makes a significant contribution to the total scattering at high energy and very small angles, the evidence of *DS* has been observed at photon energies as low as 0.889 MeV which is well below the pair production threshold [96] and at angles as high a 135°. As mentioned earlier, the scattering amplitudes for *DS* is not known for arbitrary ω and θ, limited results valid at certain ranges are available [8-10]. The Rayleigh scattering (*RS*) effect, which contributes significantly to the scattering cross section at X-ray energies, is negligible at energies > 10 MeV.

It is worth mentioning here that for a fixed value of momentum transfer Δ, $Sin\theta \propto 1/\omega$, and therefore, preferably low values of ω would allow us to consider a larger scattering angles. But, ω should not be so low that the *DS* cease to exist as the major contributor to the total scattering. For lower energies one can estimate the flux by involving other elastic scattering reactions such as Rayleigh, nuclear Thomson and nuclear resonance scatterings apart from *DS*.

It is to be noted that in obtaining eqn (5.1) and (5.3) the so called Coulomb correction (CC) effect have been neglected. Inclusion of CC at low γ-ray energies increases the DS cross section up to about 10 % whereas at high energies it slightly decreases the cross section at small momentum transfers.

It can be emphasized here that the present work is very simple and it needs some refinements to make it more realistic. But, the motivation is to make it known that the Delbrück scattering is a phenomenon which cannot be overlooked as an effect in astrophysical processes.